A Study of the Use of Contact Loading to Simulate Low Velocity Impact

Final Report

NASA Grant No. NASA NCC8-23

Prepared by

Alton L. Highsmith
Department of Aerospace Engineering
The University of Alabama

Submitted to

Frank E. Ledbetter
EH33
NASA MSFC

ABSTRACT

Although numerous studies on the impact response of laminated composites have been conducted, there is as yet no agreement within the composites community on what parameter or parameters are adequate for quantifying the severity of an impact event. One of the more interesting approaches that has been proposed uses the maximum contact force during impact to "quantify" the severity of the impact event, provided that the impact velocity is sufficiently low. A significant advantage of this approach, should it prove to be reliable, is that quasi-static contact loading could be used to simulate low velocity impact. In principle, a single specimen, loaded quasi-statically to successively increasing contact loads could be used to map the entire spectrum of damage as a function of maximum contact force. The present study had as its objective assessing whether or not the maximum contact force during impact is a suitable parameter for characterizing an impact.

The response of $[\pm 60/0_4/\pm 60/0_2]_s$ laminates fabricated from Fiberite T300/934 graphite epoxy and subjected to quasi-static contact loading and to low velocity impact was studied. Three quasi-static contact load levels -- 525 lb., 600 lb., and 675 lb. -- were selected. Three impact energy levels -- 1.14 ft.-lb., 2.0 ft.-lb., and 2.60 ft.-lb. -- were chosen in an effort to produce impact events in which the maximum contact forces during the impact events were 525 lb., 600 lb., and 625 lb., respectively. Damage development was documented using dye-penetrant enhanced x-ray radiography. A digital image processing technique was used to obtain quantitative information about the damage zone.

Although it was intended that the impact load levels produce maximum contact forces equal to those used in the quasi-static contact experiments, larger contact forces were developed during impact loading. In spite of this, the damage zones developed in impacted specimens were smaller than the damage zones developed in specimens subjected to the corresponding quasi-static contact loading. The impacted specimens may have a greater tendency to develop fiber fracture, but, at present, a quantitative assessment of fiber fracture is not available.

In addressing whether or not contact force is an adequate metric for describing the severity of an impact event, the results of this study suggest that it is not. In cases where the quasi-static load level and the maximum contact force during impact were comparable, the quasi-statically loaded specimens consistently developed larger damage zones. It should be noted, however, that using quasi-static damage data to forecast the behavior of impacted material may give conservative estimates of the residual strength of impacted composites.

Introduction

In recent years, continuous fiber reinforced composite materials have seen increasing use in advanced structural applications because of the significant weight savings they offer when compared to more traditional engineering materials. Since the material and fabrication costs of composite components are often much higher than the material and fabrication costs of metal components, composites have seen the most use in high performance structures, where weight savings significantly reduce the lifetime cost of structure. One area in which such applications are abundant is high performance transportation systems. In aircraft and high speed rail systems, reductions in vehicle structural weight reduce fuel costs and/or increase payload throughout the life of the vehicle. Rocket motor cases are also excellent candidate composite structures, as structural weight reductions translate into increased payload per launch. Composite rocket motor cases have the additional advantage that they can be formed via filament winding, a process which is relatively inexpensive in comparison to other composite fabrication techniques.

One of the difficulties that arises when polymer matrix composite materials are used for structural applications is that these materials exhibit rather brittle behavior. These materials can develop significant amounts of internal damage during a seemingly minor load excursion, such as a low velocity impact. Low velocity impacts, which may occur during the routine handling of a rocket motor case, may cause extensive ply cracking, delamination, and even fiber fracture, while few symptoms of the underlying damage state are visible at the surface of the component. It is therefore critical that the process by which damage develops in a composite subjected to low velocity impacts be understood.

Numerous studies of impact damage development in fiber reinforced composites have been presented in the literature. As yet, the composites community has not agreed upon a parameter for quantifying the severity of an impact. One of the more interesting approaches uses the maximum contact force during impact to "quantify" the severity of the impact event, provided that the impact velocity is sufficiently low. A significant advantage of this approach, should it prove to be reliable, is that quasi-static contact loading could be used to simulate low velocity impact. In principle, a single specimen, loaded quasi-statically to successively increasing contact loads could be used to map the entire spectrum of damage as a function of maximum contact force. This would allow for a very efficient use of test specimens in determining such a spectrum.

The present effort had as its objective assessing the use of quasi-static contact loading to simulate low velocity impact loads. The focus of this effort was to evaluate damage development in laminated graphite/epoxy specimens subjected to quasi-static contact loading and impact loading. In particular, the correspondence between the maximum contact force during either quasi-static loading or low velocity impact was studied. Graphite/epoxy coupons having a stacking sequence of $[\pm 60/0_4/\pm 60/0_2]_s$ were subjected to both quasi-static contact loading and low velocity impacts. Damage development was monitored via dye penetrant enhanced x-ray radiography. Radiographic images were digitized, and the damage areas were quantified.

The results of the present study indicate that for a given maximum contact force, more damage is developed during quasi-static loading than during low velocity impact. Thus, maximum

contact force is not in and of itself adequate to define the extent of the damage associated with a low velocity impact. However, using quasi-static contact loading data does provide a conservative estimate of the damage state, since more damage developed under quasi-static conditions than under dynamic loading for a given maximum contact force.

BACKGROUND

The response of polymer matrix composites to impact loads has long been a topic of interest within the composites community. Reports of such studies date back to at least the early 1970's [1-3]. The post impact performance of composites under compressive loading has probably received the most attention. The focus on compressive performance is understandable since impact induced delaminations subdivide a composite laminate into several sublaminates, and thus local buckling can occur under subsequent compressive loading. This local sublaminate buckling can lead to significant reductions in compressive performance [4]. In some structures, particularly pressure vessels such as compressed gas bottles and rocket motor cases, the load experienced by the composite is predominantly tensile.

A number of investigations have reported on the damage state that develops in a composite as a result of impact loading. A sampling of such papers is included in the list of references [5-9]. In general, there is some impact energy threshold below which a composite develops no detectable microstructural damage. This threshold varies with both the material system and the stacking sequence. For the most part, the damage that does develop when the energy threshold is exceeded is matrix damage, specifically matrix ply cracking and delamination. The size of the damaged zone is typically observed to increase with distance through the thickness from the point of impact. This observation has been made for both point and line impact loadings. To date, however, efforts to quantify the impact damage have been limited.

Since some composite structures, such as rocket motor cases, tend to be quite large, and thus prohibitively expensive to use for an extensive test program, a number of researchers have pursued concepts that make the evaluation of post impact performance more cost effective. One such area of study has been the use of quasi-static contact loading to simulate low velocity impact. The fundamental assumption behind this approach is that at sufficiently low velocities, the impact load is for all practical purposes a quasi-static event, and thus the magnitude of the contact force dictates the resulting damage state [10-13]. If quasi-static indentation can be used to simulate impact loading, then by applying progressively increasing quasi-static loads to a single specimen, the damage state as a function of contact force can be determined. In these studies, quasi-static loading has been found to simulate impact loading reasonably well, provided the impact velocity is sufficiently low [11]. However, accurate quantitative assessments of the resulting damage states were not performed.

EXPERIMENTAL PROCEDURE

Four flat laminated plates having a geometry of 48 in. by 48 in. and fabricated from Fiberite T300/934 graphite epoxy pepreg tape were provided by NASA MSFC. The laminated plates had a stacking sequence of $[\pm 60/0_4/\pm 60/0_2]_s$, where the 0° plies represent hoop direction

layers in a filament wound rocket motor case, and the $\pm 60°$ plies represent helical layers within a filament wound case. Two plates were cut into 11 in. by 3 in. coupons with their major axes aligned with the 0° direction (Type III specimens), while the other two plates were cut into 11 in. by 3 in. coupons with their major axes aligned with the 90° direction (Type IV specimens). The directions of the major axes in the two types of specimens represent the hoop and axial directions in a filament wound rocket motor case. The specimens had a nominal thickness of about 0.115 in.

Quasi-Static Contact Loading

In order to perform the quasi-static contact loading experiments, two fixtures which allow a specimen to be held in place within a servohydraulic testing machine equipped with wedge-action grips were fabricated. The first fixture, which is shown schematically in Fig. 1, holds the specimen in place. The specimen is clamped between the two top plates of the assembly via four bolts. The bolts were tightened to a torque of 90 in.-lb. in order to provide consistent clamping from experiment to experiment. These top plates contain central 2.5 in. diameter circular holes, which permit the specimen the freedom to deflect. The bottom piece of the fixture is equipped with a tang which can be held by the wedge action grips. The second fixture, the indenter fixture, is shown schematically in Fig. 2. This fixture consists of a base, which is equipped with a tang for gripping, and an indenter which is machined with a 0.5 in. diameter hemispherical contacting surface.

Contact loading experiments were performed using a computer controlled SATEC 25 Kip servohydraulic testing machine. This testing machine was equipped with hydraulic wedge-action grips. During a contact loading experiment, the specimen fixture was held in the lower grip in order to simplify the process of inserting a specimen. Thus, the specimen fixture moved with the actuator during loading. The indenter fixture, which was held in the top grip, was held fixed during the experiment.

After inserting a specimen in the specimen fixture and tightening the bolts to a torque of 90 in-lbs., the specimen fixture was raised manually until the indenter was near but not contacting specimen. A loading program written using software provided with the testing machine was then used to raise the specimen fixture under displacement control at a rate of 1 in./min. until the indenter contacted the specimen with a force of about 10 lb. Then, the specimen was loaded under load control at a rate of 600 lb./min. up to the target load, and subsequently unloaded at 600 lb./min. Once the contact force was reduced to 10 lb., the specimen fixture was lowered under displacement control at a rate of 36 in./min. to a location which gave adequate room for removing the specimen. Load and displacement data were acquired the load controlled portions of the test, but not during the displacement controlled portions of the test.

In order to determine suitable quasi-static load levels, several specimens were subjected to a series of increasing quasi-static loads. After each loading, the damage state was evaluated using the dye penetrant enhanced x-ray radiographic method discussed below. These preliminary experiments indicated that a significant fraction of the specimens developed no observable damage at loads below 500 lb. In addition, a significant faction of the specimens were penetrated by the indenter when subjected to contact loads of 700 lb. Based on these observations, three

quasi-static load levels -- 525 lb., 600 lb., and 675 lb. -- were selected for the remainder of the study.

Impact Loading

All impact tests were conducted on a Dynatup Model 8200 drop weight impact tower. An instrumented 0.5 in diameter hemispherical impacting tup was used for all experiments. The crosshead/tup assembly had a nominal weight of 9.75 lb. Adjusting the drop height adjusted the impact energy. During impacting, the specimen was held in place by a pneumatically operated clamping fixture. The specimen fixture is shown schematically in Fig. 3. As with the quasi-statically loaded specimens, a 2.5" circular region centered on the specimen was free to deflect laterally. A computer data acquisition system recorded the contact load as a function of time, as well as the impact velocity. Associated computer software determined the impact energy and the energy absorbed by the specimen from this raw data.

In order to specify impact energy levels which would give approximately the same contact loads that were used in quasi-static testing, an estimate of the specimen stiffness during transverse loading was required. Load versus deflection data from the quasi-static tests were used to obtain this information. The impact energy levels were determined by integrating the areas under the load-deflection curves from the quasi-static tests from zero load to the maximum contact load. The three impact energy levels determined in this fashion were approximately 1.14 ft.-lb., 2.00 ft.-lb., and 2.60 ft.-lb.

Dye-Penetrant Enhanced X-Ray Radiography

After quasi-static or impact loading, a region on the back surface of each specimen opposite the point of contact was encircled by a small dam fashioned from plumber's putty. This dam was then filled with a zinc iodide dye penetrant solution (60 g ZnI, 10 ml water, 10 ml isopropyl alcohol, 10 ml Kodak "Photo-Flo 200"). The dye penetrant was allowed to soak into the specimen for a minimum of 24 hours. The dye penetrant decorated those damage events (matrix cracks, delaminations, etc.) into which it could flow, and rendered those damage events more opaque to x-rays than the surrounding undamaged material.

Three radiographs were taken of each specimen using different angles of incidence for the incoming x-ray beam -- one with an angle of incidence of 82.5°, one with an angle of incidence of 90°, and one with an angle of incidence of 97.5°. The configurations used for obtaining these three radiographic views are shown schematically in Fig. 4. The 90°, or normal incidence, x-ray view provided a "planform view" of damage within the specimen. The other two views formed a stereoscopic x-ray pair. When such a stereo pair is viewed using a stereo viewer, a three dimensional image of the distribution of damage within the segment can be seen [14]. This procedure was used to resolve the location of specific damage events through the thickness of the specimen.

Digital Image Processing of Radiographs

In an effort to obtain some quantitative measures of the damage state to facilitate comparisons between the different specimens, a simple image processing scheme developed by the author of this paper was employed. Normal incidence x-ray radiographs were digitized using a

flat bed scanner. Digitized versions of each radiograph were stored as binary bitmap files, specifically as Tagged Image File Format (TIFF) files. A computer program written in C++ was then used to analyze the images. The first step of this analysis was to identify those pixels within the digitized image that corresponded to damaged regions within the composite. A search routine identified those pixels that were darker than a user selected gray scale (i.e., pixels associated with dye penetrant decorated damage), as well as those pixels contained within a continuous group of pixels darker than the user selected threshold. A new image was produced in which all pixels associated with damaged areas were set to black, while the remaining pixels were set to white. A commercial TIFF viewer could then be used to compare the selected pixels with the original image, and thus help guide the selection of the gray level threshold.

A typical radiograph, one obtained from specimen III-4, is shown in Fig. 5a. The corresponding modified image obtained by processing the digitized form of the radiograph in Fig. 5a is shown in Fig. 5b . The correlation between the selected points which have been set to black in Fig. 5b and the damaged regions of the radiograph of Fig. 5b is quite good. It should be noted that while the delaminated region dominates Fig. 5b, some damage outside the delaminated zone is also identified. At present, no attempt has been made to filter features such as ply cracks located outside the bounds of the delaminated area out of the modified image.

After identifying those pixels associated with damage, the identified pixels were counted, and thus the net projected damage area was determined. The centroid of the damaged area was also calculated. Finally, the second moments of the identified damage area were calculated with respect to a centroidal coordinate system. The following definitions of these second moments of area were used:

$$I_{xx} = \int_A x^2 dA \qquad I_{yy} = \int_A y^2 dA \qquad I_{xy} = \int_A xy dA$$

where the x axis is the direction of the 0° fibers, and the y axis is the transverse axis. These definitions differ from the definitions of the area moments of inertia used in most strength of materials texts.

RESULTS

525 Lb. Quasi-Static Load

The 525 lb. quasi-static load level represented a threshold level for inducing damage via contact loading. Of the five type III specimens and five type IV specimens that were loaded to 525 lb. and inspected radiographically, 3 specimens showed no detectable impact damage. Four others showed tiny amounts of matrix damage. A sample radiograph taken from one of these specimens, specimen III-30, is presented in Fig. 6. The dominant damage feature is a ply crack in 0o layers nearest the back side of the specimen (farthest away from the point of contact loading thickness). This ply crack runs in the horizontal direction in Fig. 6. There is also some indication of a small amount of delamination. The last three of the specimens exhibited more significant damage zones. A radiograph taken from Specimen IV-27 presented in Fig. 7 shows such a damage pattern. It should be noted that the type IV specimens were cut from the panels with

their long dimension perpendicular to the primary load carrying direction, the 0° direction. Thus, where the 0° direction appeared as the horizontal direction in Fig. 6, it appears in the vertical direction in Fig. 7. The damage state seen in Fig. 7 includes ply cracking in plies of all three ply orientations -- 0°, 60°, and -60°. In addition, delamination has developed at a numerous ply interfaces through the laminate thickness.

Table 1 summarizes the basic data obtained from the from the experiments in which the specimens were loaded to 525 lb. It can be seen that in fact, the peak contact load exceeded the 525 lb. target, albeit only by a few pounds. The damage zone sizes, which represent primarily projected delamination area, range from no visible damage up to damage zones of 0.446 $in.^2$. Clearly, the 525 lb. load level represents a transition between load levels which cause no damage and load levels which cause significant damage.

600 Lb. Quasi-Static Load

Two representative radiographs taken from specimens subjected to 600 lb. quasi-static contact loads are shown in Fig. 8. The radiograph of specimen III-21, which developed on of the smaller damage zones of the specimens subjected to this load level, is shown in Fig 8a, and the radiograph of specimen IV-44, which developed on of the larger damage zones of the specimens subjected to this load level, is shown in Fig 8b. Qualitatively, the damage patterns are quite similar. Ply cracking can be seen in plies of all three ply orientations. The delaminated areas are not quite circular. In addition, both radiographs show large "lobes" of delamination which appear to radiate out from the contact point in the 60° direction. These large delaminations developed near the back surface of the specimen.

Test data compiled from the specimens subjected to the 600 lb. quasi-static contact load is presented in Table 2. Once again, the actual peak contact loads exceeded the 600 lb. target, typically by a few pounds. Damage areas vary from a low of 0.466 $in.^2$ to a high of 0.862 $in.^2$. In addition, the second moment of the damage area with respect to the 0° coordinate (x) is consistently larger than the second moment of the damage area with respect to the transverse coordinate (y). This indicates that the damage zones are longer in the 0° direction than they are in the transverse direction. The products of inertia are quite small in all cases, indicating that the damage zone is nearly symmetric. As a final note, the damage areas observed in specimens loaded to 600 lb. were larger than the damage areas observed in specimens loaded to 525 lb.

675 Lb. Quasi-Static Load

The 675 lb. quasi-static contact load was a load level very near the limit load for his material. Of the ten specimens subjected to the 625 lb. contact load, two failed during loading. These failures occurred when the indenter penetrated the specimens, and, in essence, punched a hole through the specimens. An radiographic inspection of damage performed on those specimens that survived the loading showed significant amounts ply cracking, as well as the development of rather large delaminations. In addition, fiber fracture was observed. A typical radiograph, one obtained from specimen III-47, is shown in Fig. 9. Visible in the radiograph is a set of especially dark, somewhat broad lines which closely surround the point of contact. These

lines contain fiber fracture in both the 0° and 60° plies. Figure 10 contains a radiograph of specimen IV-43, the most severely damaged of the surviving specimens. Large lobes of delamination are seen to have grown from the point of contact along a 60° line, an indication the penetration of the indenter was eminent. Again, there is evidence of fiber fracture in the 0° and 60° layers in the vicinity of the impact site.

A summary of the test data is provided in Table 3. Damage areas in the surviving specimens ranged from 0.630 $in.^2$ to 0.917 $in.^2$. As a group, the specimens loaded to 675 lb. developed larger damage zones than those subjected to 600 lb., although there was some overlap between these two groups of specimens. For the most part , $I_{xx}>I_{yy}$, and, with three exceptions in which the growth of the 60° lobes of delamination was quite pronounced, I_{xy} is quite small, indicating symmetry of the damage zone.

Low energy Impact

Data from the low energy (1.14 ft.-lb. nominal) impact specimens is summarized in Table 4. The maximum contact loads developed during the low energy impact experiments were consistently higher than the 525 lb. that was intended. This indicates that the specimens are "stiffer" during dynamic loading than they are during quasi-static loading. Damping and inertia effects contribute to this increased "stiffness". The maximum contact loads achieved during the low level impact experiments were, as a rule, higher than those achieved during the 525 lb. quasi-static loading (Table 1). However, only two of the ten impacted specimens developed detectable damage. Further, no impacted specimens developed the significant damage zones observed in three of their quasi-statically loaded counterparts.

Medium Energy Impact

Data from the medium impact energy (2.00 ft.-lb. nominal) impact specimens is summarized in Table 5. It cab be seen that although the impact energies were slightly lower than target value, most of the maximum contact forces were significantly larger than the intended value of 600 lb. Further, in spite of these higher contact forces, the damage zones developed under impact loading were smaller than those developed in specimens loaded quasi-statically to 600 lb. (Table 2). The second moments of the damage area indicate that generally, the delaminated zones are longer in the 0° direction than they are in the transverse direction, and that the damage zones are by and large symmetric.

A typical radiograph is shown in Fig. 11. The damage state is qualitatively similar to the that observed in the specimens subjected to 600 lb. quasi-static loads. In a few of the impacted specimens, however, there was evidence of fiber fracture. Fig. 12 shows a radiograph obtained from specimen IV-33, the medium energy impact specimen that experienced the highest maximum contact load. A vertical line can be seen emanating upward from the point of impact. This feature is not straight, but in fact has some curvature. A microscopic inspection of the radiograph revealed this feature to be a stair-step pattern of fiber fracture in a 60° layer.

High Energy Impact

Data from the high impact energy (2.60 ft.-lb. nominal) impact specimens is summarized in Table 6. For most of the specimens, maximum contact forces were larger than the intended value,

which was 675 lb. However, for three specimens, the maximum contact force was lass than the 675 lb. target value. All of these impacted specimens developed damage zones which were smaller than 0.630 $in.^2$, the smallest damage zone observed in a specimen loaded quasi-statically to 675 lb. (see Table 3). As a group, these specimens did develop larger damage zones than those observed in the specimens subjected to the medium energy impact, but there is overlap between the two groups. Once again, the second moments of the damage areas indicate that the delaminated zones are longer in the 0° direction than they are in the transverse direction, and that the damage zones are essentially symmetric.

A representative radiograph obtained from a specimen subjected to a high energy impact is shown in Fig. 13. The usual pattern of ply cracking and delamination are readily visible. In addition, stair step patterns of fiber fracture in the 0° and 60° layers can be seen in the intensely damaged regions surrounding the impact site. It should be noted that none of the specimens subjected to the high energy impact developed fiber fracture as pronounced as that observed in specimen IV-33, which was subjected to a medium energy impact. However, as a group, specimens subjected to high energy impacts exhibited more fiber fracture than did specimens subjected to medium energy impacts.

SUMMARY AND CONCLUSIONS

In this research program, the response of $[\pm 60/0_4/\pm 60/0_2]_s$ graphite epoxy laminates subjected to quasi-static contact loading and to low velocity impact was studied. Three quasi-static contact load levels -- 525 lb., 600 lb., and 675 lb. -- were selected. Three impact energy levels -- 1.14 ft.-lb., 2.0 ft.-lb., and 2.60 ft.-lb. -- were chosen in an effort to produce impact events in which the maximum contact forces during the impact events were 525 lb., 600 lb., and 625 lb., respectively. Damage development was documented using dye-penetrant enhanced x-ray radiography. A digital image processing technique was used to obtain quantitative information about the damage zone.

Considering first the quasi-statically loaded specimens, increasing the load generally resulted in an increased damage area. There was, however, significant scatter within a given group of specimens subjected to the same load. The dominant features seen in the radiographs were ply cracks and delaminations. The 525 lb. quasi-static load level was a threshold level, since some specimens subjected to this load level developed damage, while others did not. The 675 lb. load was very near the failure load, and in fact two specimens failed during this loading. Some specimens that survived the 675 lb. load did exhibit fiber fracture in the various constituent layers.

Although it was intended that the impact load levels produce maximum contact forces equal to those used in the quasi-static contact experiments, larger contact forces were developed during impact loading. In spite of this, the damage zones developed in impacted specimens were smaller than the damage zones developed in specimens subjected to the corresponding quasi-static contact loading. The impacted specimens may have a greater tendency to develop fiber fracture, but, at present, a quantitative assessment of fiber fracture is not available.

In addressing whether or not contact force is an adequate metric for describing the severity of an impact event, the results of this study suggest that it is not. In cases where the quasi-static load level and the maximum contact force during impact were comparable, the quasi-statically loaded specimens consistently developed larger damage zones. It should be noted, however, that since larger damage zones were developed under quasi-static loading, using quasi-static damage data to forecast the behavior of impacted mateial may in fact give conservative estimates of residual strength. Thus, quasi-static indentation data may still prove useful for predicting the post-impact performance of laminated composites.

REFERENCES

[1] Toland, R.H., "Impact Testing of Carbon Fibre Composite Materials," ASTM STP 569, American Society for Testing and Materials, Philadelphia, 1973, pp.133-145.

[2] Rogers, K.F., Sidney, G.R., and Kingston-Lee, M.D., "Ballistic Impact Resistance of Carbon Fibre Laminates," Composites, Vol. 2, December 1971, pp.237-241.

[3] Staines, J.H., Rhodes, M.D., and Williams, J.G., "Effect of Impact Damage and Holes on the Comressive Strength of a Graphite/Epoxy Laminate," ASTM STP 696, American Society for Testing and Materials, Philadelphia, 1976, pp.145-171.

[4] Whitcomb, J.D., "Delamination Growth in a Laminate with a Postbuckled Edge Delamination," J. Composites Technology and Research, Vol. 13, pp. 175-178.

[5] Gerszczuk, L.B. and Chao, H., "Impact Damage in Graphite Fiber Composites," ASTM STP 617, 1977, pp. 389-408.

[6] Meyer, P.I., "Low Velocity Hard-Object Impact of Filament-Wound Kevlar Epoxy Composite," Composites Science and Technology, Vol. 33, 1988, pp. 279-293.

[7] Srnivasan, K., Jackson, W.C., Smith, B.T., and Hinkley, J.A., "Characterization of Damage Modes in Impacted Thermoset and Thermoplastic Composites," J. Reinforced Plastics and Composites, Vol. 11, 1992, pp. 1111-1126.

[8] Choi, H.Y., Downs, R.J., and Chang, F.-K., "A New Approach toward Understanding Damage Mechanisms and Mechanics of Laminated Composites Due to Low Velocity Impact: Part I - Experiments," J. Composite Materials, Vol. 25, 1991, pp. 992-1011.

[9] Choi, H.Y., Wang, H.S., and Chang, F.K., "Effect of Laminate Configuration and Impactor's Mass on the Initial Damage of Graphite/Epoxy Composite Plates Due to Line Loading," J. Composite Materials, Vol. 26, 1992, pp. 804-827.

[10] Poe, C.C., Jr., "Simulated Impact Damage in a Thick Graphite/Epoxy Laminate Using Spherical Indenters," J. Reinforced Plastics and Composites, Vol. 10, 1991, pp. 293-307.

[11] Jackson, W.C. and Poe, C.C., Jr., "The Use of Impact Force as a Scale Parameter for the Impact Response of Composite Laminates," J. Composites Technology and Research, Vol 15, Winter 1993, pp. 282-289.

[12] Cairns, D.S., "A Simple Elasto-Plastic Contact Law for Composites," J. Reinforced Plastics and Composites, Vol. 10, 1991, pp. 423-433.

[13] Kwon, Y.S. and Sankar, B.V., "Indentation-Flexure and Low-Velocity Impact Damage in Graphite Epoxy Laminates," J. Composites Technology and Research, Vol. 15, pp. 101-111.

[14] Jamison, R.D., "Advanced Fatigue Damage Development in Graphite Epoxy Laminates," Ph.D. Dissertation, Virginia Polytechnic Institute and State University, Aug. 1982.

Table 1. Load and quantitative damage state data from specimens subjected to a 525 Lb. nominal quasi-static contact load.

Specimen	Contact Load (Lbs.)	A (in.^{4})	I_{xx} (in.^{4})	I_{yy} (in.^{4})	I_{xy} (in.^{4})
III-13	540.370		No detectable damage		
III-58	539.740	0.446	0.022	0.012	0.000
III-10	531.410	0.005	0.000	0.000	0.000
III-30	529.230	0.026	0.000	0.001	0.000
III-19	529.700	0.377	0.014	0.010	0.000
IV-27	536.940	0.418	0.017	0.012	0.001
IV-21	533.200		No detectable damage		
IV-7	531.100	0.002	0.000	0.000	0.000
IV-35	532.740	0.015	0.000	0.000	0.000
IV-18	533.130		No detectable damage		

Table 2. Load and quantitative damage state data from specimens subjected to a 600 Lb. nominal quasi-static contact load..

Specimen	Contact Load (Lbs.)	A (in.^{4})	I_{xx} (in.^{4})	I_{yy} (in.^{4})	I_{xy} (in.^{4})
III-35	615.880	0.891	0.105	0.061	-0.013
III-21	606.770	0.566	0.031	0.024	0.006
III-18	610.740	0.605	0.034	0.028	0.003
III-4	606.770	0.466	0.023	0.014	-0.001
III-2	604.830	0.580	0.036	0.021	0.000
IV-14	621.720	0.500	0.026	0.017	0.000
IV-44	603.190	0.853	0.067	0.053	0.003
IV-10	608.950	0.496	0.023	0.018	0.001
IV-24	604.590	0.539	0.028	0.020	0.001
IV-36	606.930	0.714	0.049	0.035	-0.001

Table 3. Load and quantitative damage state data from specimens subjected to a 675 Lb. nominal quasi-static contact load..

Specimen	Contact Load (Lbs.)	A (in.^{4})	I_{xx} (in.^{4})	I_{yy} (in.^{4})	I_{xy} (in.^{4})	I_{xx}/I_{yy}
III-63	680.580	0.636	0.037	0.031	-0.007	
III-62	683.690	0.756	0.057	0.039	-0.005	
III-6	673.800		Failed during quasi-static loading.			
III-47	682.370	0.669	0.047	0.029	0.004	
III-40	679.720	0.630	0.040	0.027	0.004	
IV-52	684.780	0.882	0.072	0.068	0.017	
IV-3	681.670	0.884	0.073	0.085	-0.041	
IV-48	679.250	0.719	0.049	0.037	0.003	
IV-40	640.950		Failed during quasi-static loading.			
IV-43	679.880	0.917	0.079	0.069	0.016	

Table 4. Load and quantitative damage state data from specimens subjected to low energy impact.

Specimen	Contact Load (Lbs.)	Energy Level (Ft.-Lb.)	A ($in.^4$)	I_{xx} ($in.^4$)	I_{yy} ($in.^4$)	I_{xy} ($in.^4$)
III-12	543.700	1.130	No detectable damage.			
III-27	559.870	1.130	No detectable damage.			
III-66	552.790	1.130	No detectable damage.			
III-36	567.610	1.130	No detectable damage.			
III-65	536.270	1.150	0.008	0.001	0.000	0.000
IV-63	567.610	1.140	No detectable damage.			
IV-15	554.970	1.140	0.015	0.001	0.001	0.000
IV-65	563.560	1.130	No detectable damage.			
IV-4	554.470	1.140	No detectable damage.			
IV-61	567.100	1.140	No detectable damage.			

Table 5. Load and quantitative damage state data from specimens subjected to medium energy impact.

Specimen	Contact Load (Lbs.)	Energy Level	A (in.^{4})	I_{xx} (in.^{4})	I_{yy} (in.^{4})	I_{xy} (in.^{4})
III-32	677.480	1.950	0.305	0.010	0.006	0.000
III-14	598.610	1.950	0.319	0.010	0.007	0.000
III-11	681.710	1.950	0.325	0.011	0.007	0.000
III-23	591.690	1.960	0.426	0.017	0.013	0.000
III-17	677.160	1.960	0.338	0.010	0.008	0.000
IV-25	656.240	1.980	0.324	0.019	0.004	0.001
IV-33	735.620	1.980	0.380	0.019	0.007	0.001
IV-29	680.000	1.990	0.338	0.012	0.008	0.000
IV-9	683.040	1.960	0.324	0.009	0.008	0.001
IV-26	647.830	1.960	0.314	0.010	0.007	0.000

Table 6. Load and quantitative damage state data from specimens subjected to high energy impact.

Specimen	Contact Load (Lb.)	Energy Level (Ft.-Lb.)	A (in.^{4})	I_{xx} (in.^{4})	I_{yy} (in.^{4})	I_{xy} (in.^{4})
III-61	600.290	2.610	0.318	0.010	0.008	0.003
III-42	685.760	2.600	0.403	0.018	0.011	-0.004
III-1	645.300	2.620	0.485	0.023	0.016	0.002
III-34	731.270	2.600	0.442	0.020	0.013	0.002
III-44	758.580	2.590	0.410	0.015	0.142	-0.005
IV-1	742.900	2.590	0.371	0.013	0.010	0.002
IV-20	712.050	2.600	0.302	0.009	0.006	0.001
IV-66	710.030	2.600	0.348	0.012	0.008	0.001
IV-60	645.800	2.610	0.348	0.013	0.008	0.001
IV-41	706.490	2.600	0.408	0.017	0.011	0.001

Specimen Fixture Assembly

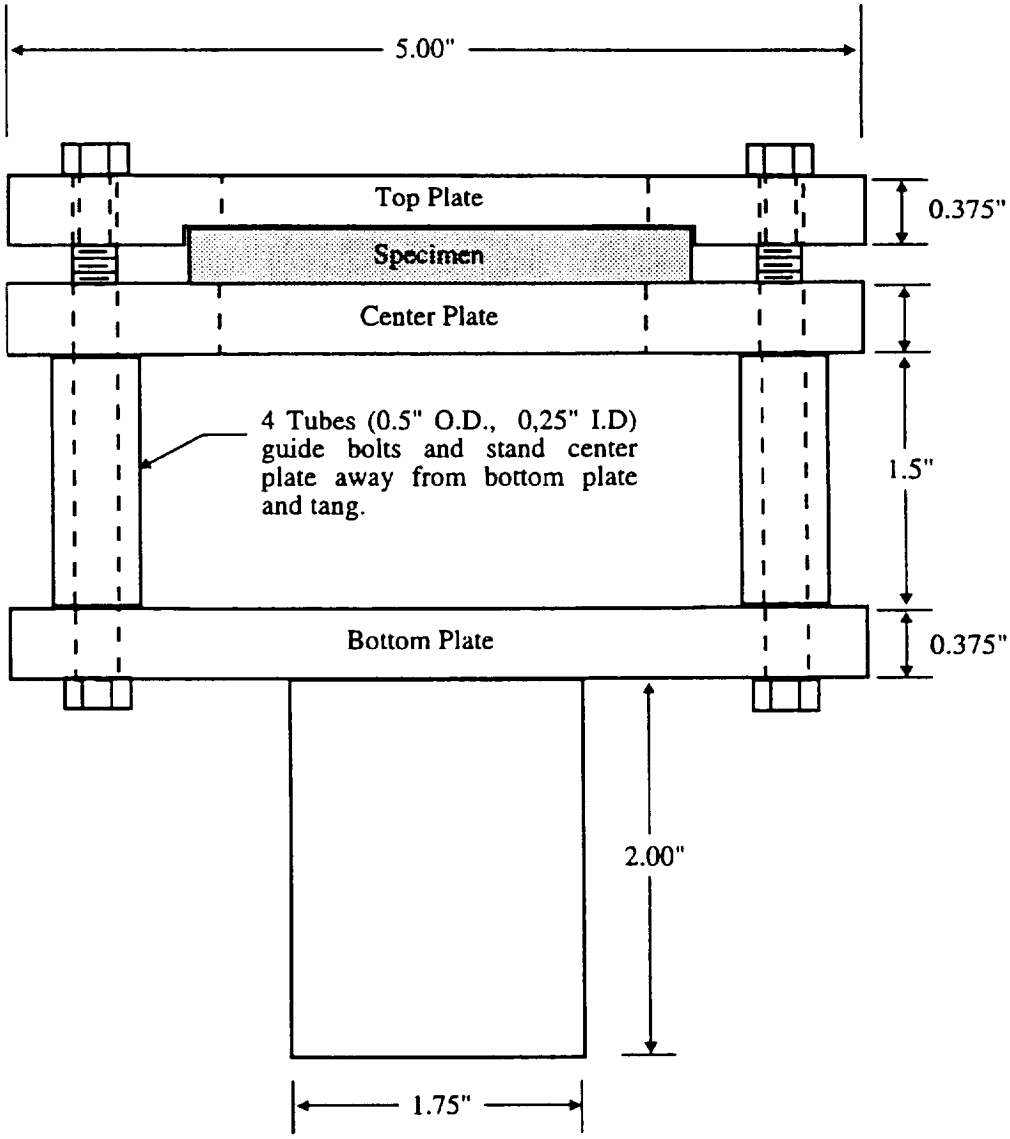

Note: All bolts 1/4-20

Figure 1. Assembly drawing of the specimen fixture used for quasi-static contact loading.

Indenter Fixture

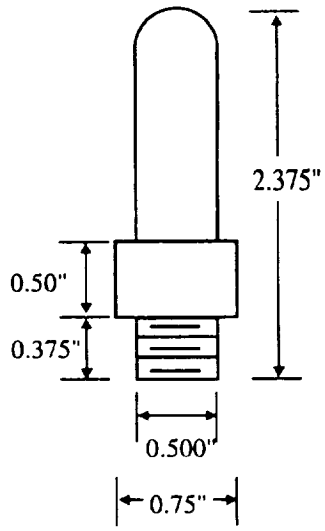

Indenter is made from 0.75" diameter stainless steel bar stock. It has a 0.5" dia. spherical tip machined on one end, and is threaded on the other. The shoulder helps seat the indenter against the tang assembly.

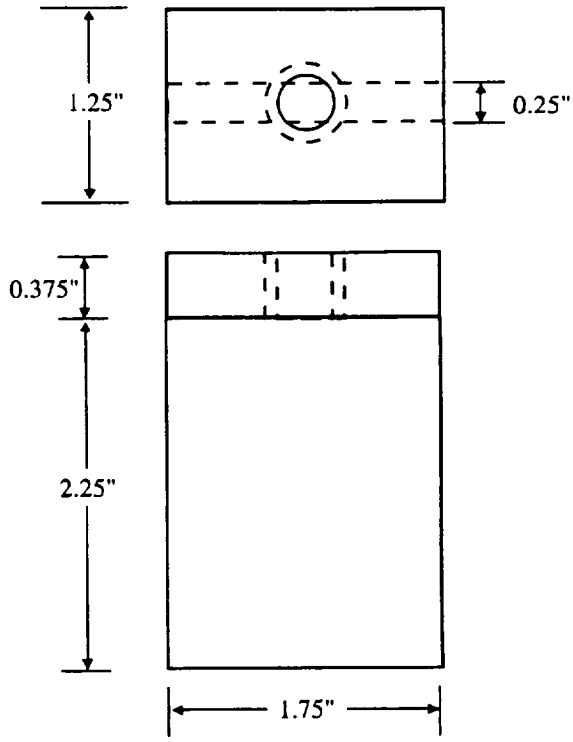

Tang requires 2.00" long flat area below fillet

Figure 2. Schematic diagram of the indenter fixture used for quasi-static contact loading.

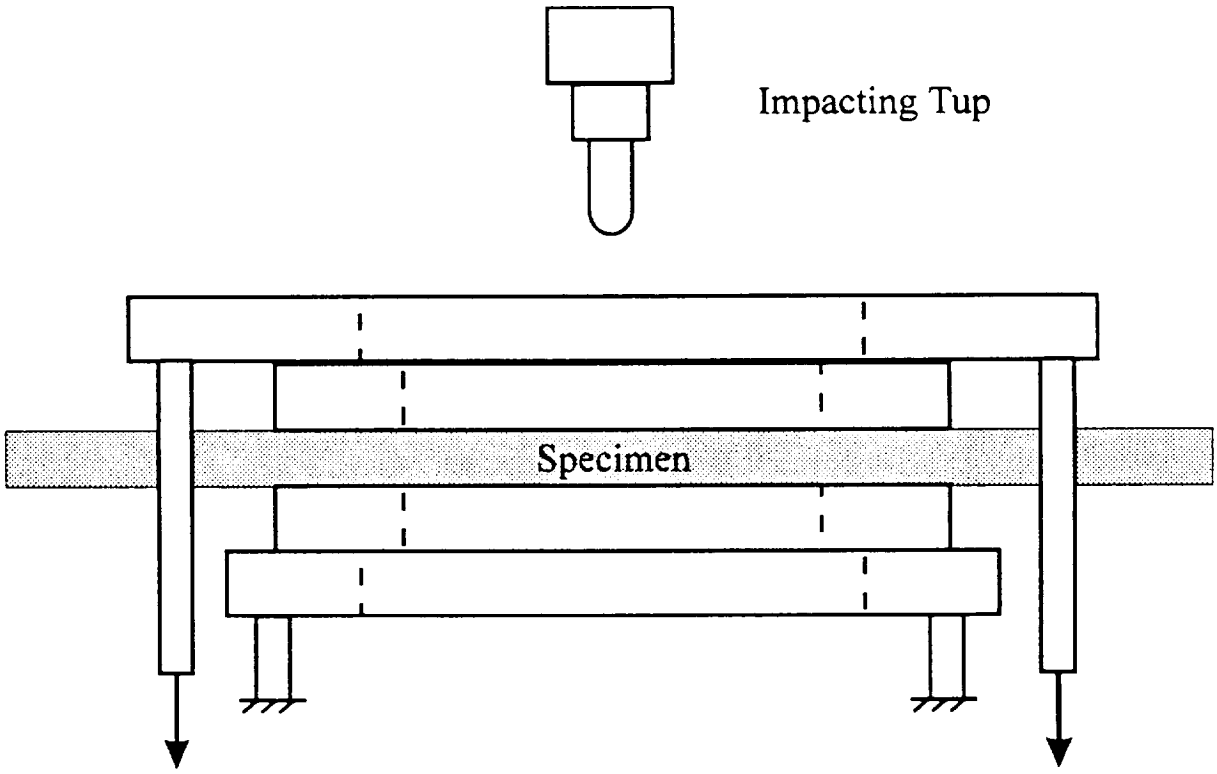

Figure 3. Schematic diagram of the specimen fixture used for impact loading.

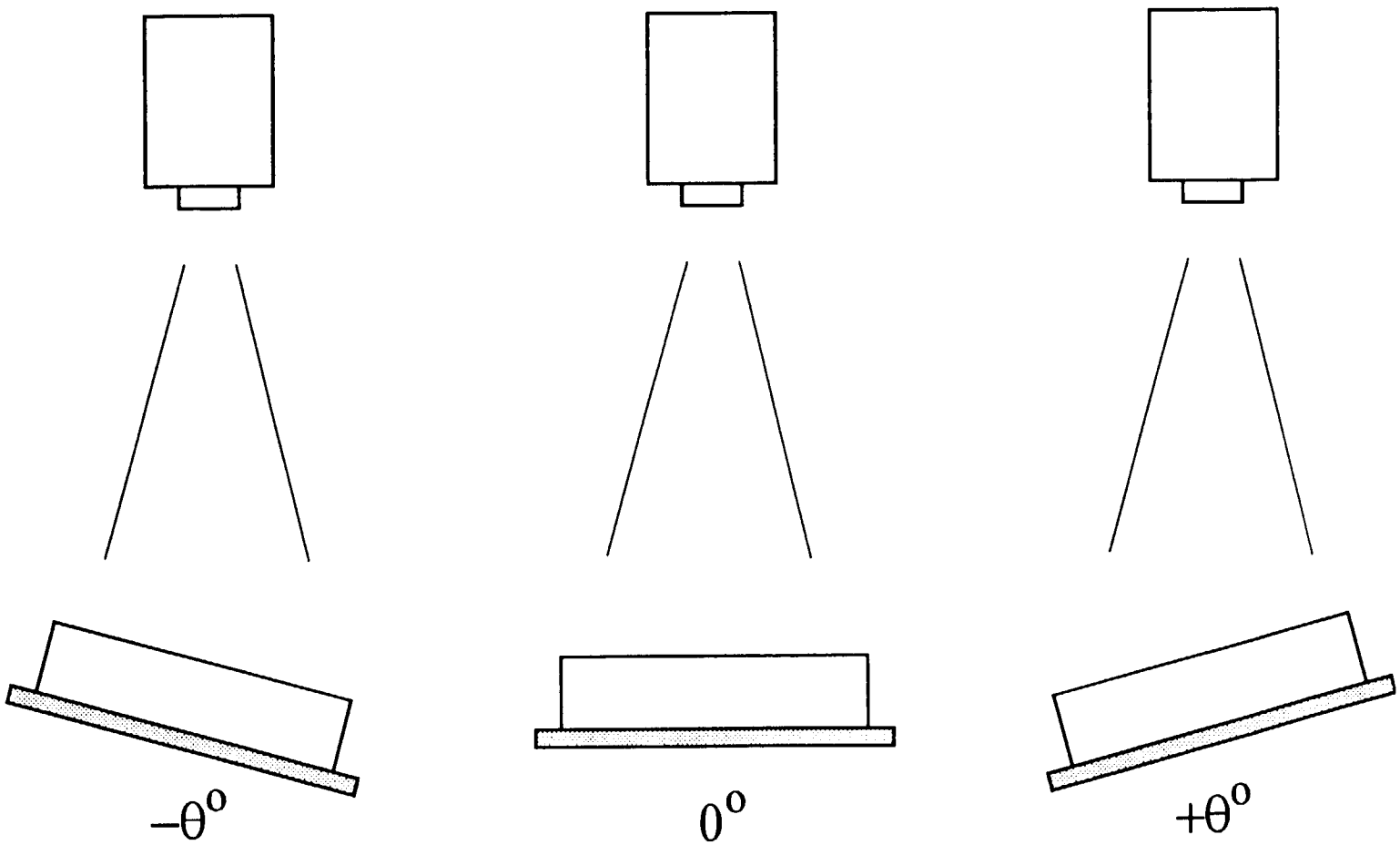

Figure 4. Schematic representation of the three x ray views used for normal incidence viewing and stero radiography.

(a)

(b)

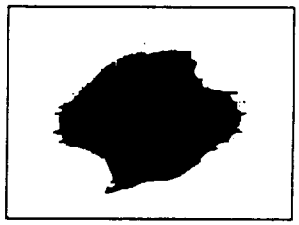

Figure 5. (a) An x-ray rdiograph of specimen III-4 and (b) the corresponding damage area detected by the digital image processing routine.

Figure 6. Dye-penetrant enhanced x-ray radiograph of specimen III-30, which had been subjected to a 525 lb. quasi-static contact load.

Figure 7. Dye-penetrant enhanced x-ray radiograph of specimen IV-27, which had been subjected to a 525 lb. quasi-static contact load.

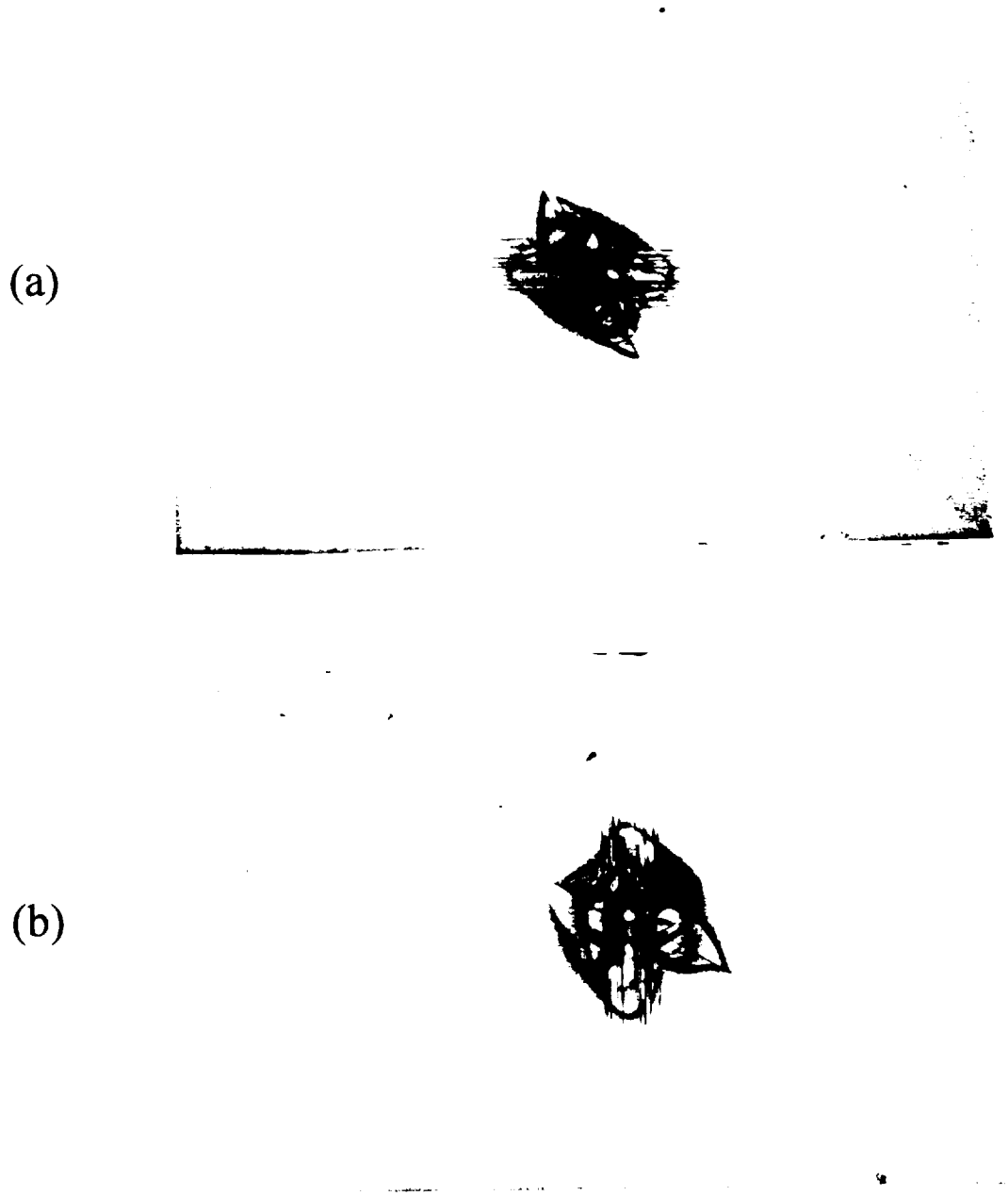

Figure 8. Dye-penetrant enhanced x-ray radiograph (a) specimen III-21 and (b) specimen IV-44, which had been subjected to 600 lb. quasi-static contact loads.

Figure 9. Dye-penetrant enhanced x-ray radiograph of specimen III-47, which had been subjected to a 675 lb. quasi-static contact load.

Figure 10. Dye-penetrant enhanced x-ray radiograph of specimen IV-43, which had been subjected to a 675 lb. quasi-static contact load.

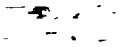

Figure 11. Dye-penetrant enhanced x-ray radiograph of specimen III-14, which had been subjected to a medium energy impact.

Figure 12. Dye-penetrant enhanced x-ray radiograph of specimen IV-33, which had been subjected to a medium energy impact.

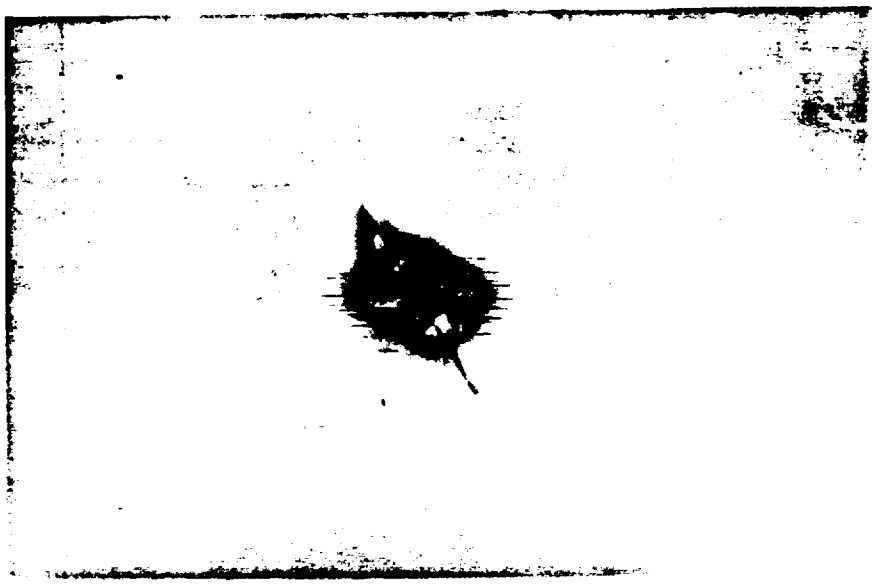

Figure 10. Dye-penetrant enhanced x-ray radiograph of specimen III-61, which had been subjected to a high energy impact.